Axial and Equatorial Hydrogen Bonds in Pentamethylene Sulfide ··· Hydrogen Chloride Complex

M. Eugenia Sanz, Juan C. López, and José L. Alonso*[a]

Abstract: Axial and equatorial hydrogen bonds have been observed in the heterodimer formed between pentamethylene sulfide and hydrogen chloride in a pulsed supersonic expansion by using Fourier transform microwave spectroscopy. The ground-state rotational spectra of the isotopic species ($C_5H_{10}{}^{32}S$, $H^{35}Cl$), ($C_5H_{10}{}^{32}S$, $H^{37}Cl$), ($C_5H_{10}{}^{32}S$, $D^{35}Cl$), and ($C_5H_{10}{}^{34}S$, $H^{35}Cl$) have been analyzed for the equatorial conformer, and the first three of these for the axial form in the frequency range 6–18 GHz. Interpretation of the rotational constants led to the conclusion that the observed complexes have C_s symmetry with the hydrogen chloride pointing to the domain of axial or equatorial lone pairs at the sulfur atom. The equatorial form has been found to be the most stable one, in contrast to the observation in the related tetrahydropyran ··· HCl complex (*Angew. Chem.* **1999**, *111*, 1889–1892; *Angew. Chem. Int. Ed.* **1999**, *38*, 1772–1774). The conformational preference is discussed in the context of second-order interactions.

Keywords: conformation analysis · hydrogen bonds · microwave spectroscopy · rotational spectroscopy

Introduction

Hydrogen bonding has been the subject of considerable research effort over the years owing to its central role in many chemical, physical, and biological phenomena.[1] The intrinsic properties of the hydrogen bond can be obtained from the study of isolated hydrogen-bonded dimers. In recent years such studies have been undertaken in the collisionless environment of supersonic jets where complexes are easily formed and can be detected by using different spectroscopic methods.[2] An important type of hydrogen-bond dimer B ··· HX (where X = F, Cl, Br, etc.) is that in which the proton-acceptor atom B (B = O, S, etc.) carries two equivalent nonbonding electron pairs. We have recently studied complexes in which B is a five-membered heterocycle, such as tetrahydrothiophene ··· HCl,[3] tetrahydrothiophene ··· HF,[4] tetrahydrofuran ··· HCl,[5] and tetrahydrofuran ··· HF[6] by using molecular beam Fourier transform microwave spectroscopy. In all cases two equivalent equilibrium conformations with pyramidal configurations at O or S have been found; the HX molecule points to the domain of one of the two equivalent nonbonding electron pairs. Such geometries are consistent with a set of empirical rules[7] enunciated to predict the structures of hydrogen-bonded complexes. However, these rules do not deal with a situation where there are nonequivalent nonbonded pairs, and thus it should be interesting to examine what happens when one attempts to apply these rules to complexes in which the acceptor molecule B carries two nonequivalent electron pairs. The six-membered rings tetrahydropyran and pentamethylene sulfide (PMS)[8, 9] fall into this category with two nonequivalent binding sites at the oxygen or sulfur atom. When complexed with HCl, the hydrogen bond would be formed to the nonbonding electron pair localized at the axial and/or equatorial position. We have recently presented the results on the tetrahydropyran ··· HCl complex[10] for which axial and equatorial forms have been observed. Parallel to this study we investigated the PMS ··· HCl heterodimer for which axial and equatorial hydrogen bond conformers such as those depicted in Scheme 1 are expected. If formed in the adiabatic expansion they would exhibit individual rotational spectra. Their analysis provides

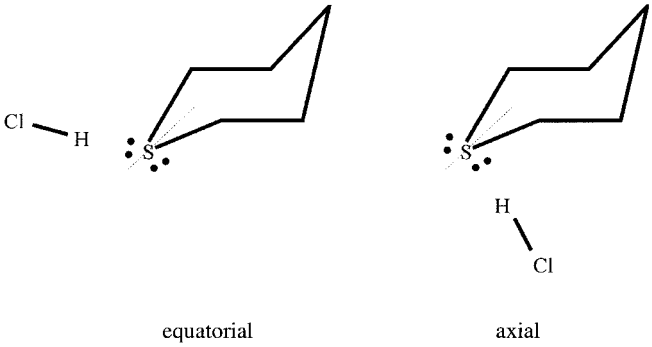

equatorial axial

Scheme 1. Axial and equatorial hydrogen bonds in pentamethylene sulfide ··· HCl.

[a] Prof. J. L. Alonso, M. E. Sanz, Prof. J. C. López
Departamento de Química Física, Facultad de Ciencias,
Universidad de Valladolid
E-47005 Valladolid (Spain)
Fax.: (+34) 983-423264
E-mail: jlalonso@qf.uva.es

Supporting information for this article is available on the WWW under http://www.wiley-vch.de/home/chemistry/ or from the author.

  0947-6539/99/0511-3293 $ 17.50+.50/0

unequivocal answers to the question of the binding sites and yields the structure of hydrogen-bonded dimers in effective isolation.

Results

Rotational spectra

From the structural models in Scheme 1 both axial and equatorial PMS···HCl conformers have a plane of symmetry containing the *a* and *b* or *c* axes of inertia. Preliminary rotational constants were estimated from the structures of PMS[8, 9] and HCl.[11] The geometrical parameters of the hydrogen bond were taken from the related tetrahydrothiophene···HCl complex[3] using a linear hydrogen bond structure. Both forms were predicted to be nearly prolate asymmetric tops with strong a-type transitions and relatively weak b- or c-type transitions.

We surveyed several regions between 6 and 18 GHz, which covered angular momentum from $J=3$ to 10. Apart from the PMS and the Ar···HCl lines used to test the gas mixture, the dominant feature of the spectra is the presence of two series of closely spaced transitions occurring approximately every 1900 and 1600 MHz which account for the B + C values of the axial and equatorial conformers. The lines were identified as μ_a, R-branch transitions of $C_5H_{10}{}^{32}S\cdots H^{35}Cl$ belonging to the families $(J+1)_{K'_{-1},K'_{+1}} \leftarrow J_{K''_{-1},K''_{+1}}$ with K_{-1} values ranging from 0 to 4. From further analysis, some weaker μ_b and μ_c R-branch transitions were assigned to the axial and equatorial conformers, respectively. In order to gain more understanding about the structures of the dimers, the isotopic species $C_5H_{10}{}^{32}S\cdots H^{37}Cl$ and $C_5H_{10}{}^{32}S\cdots D^{35}Cl$ were also measured for both axial and equatorial forms. In addition, the isotopic species $C_5H_{10}{}^{34}S\cdots H^{35}Cl$ was observed in its natural abundance for the equatorial conformer. Apart from the systematic Doppler splitting, all transitions show a hyperfine structure owing to the nuclear quadrupole coupling with the Cl nucleus (both ^{35}Cl and ^{37}Cl have $I=3/2$). The ^{35}Cl nuclear quadrupole splitting is illustrated in Figure 1 which gives an overview of the $5_{0,5} \leftarrow 4_{0,4}$ transition for the equatorial form. Since the hyperfine splitting is large enough, the lines were assigned in terms of the coupling scheme $\boldsymbol{J}+\boldsymbol{I}=\boldsymbol{F}$. Table 1 and 2 show a selection of the measured transitions. In all cases the lines corresponding to the equatorial conformer were found to be more intense (about three or four times) than those for the axial form in either Ar or He as carrier gases.

For each isotopomer the analysis of the rotational data was based on the Hamiltonian $\boldsymbol{H}=\boldsymbol{H_R}+\boldsymbol{H_Q}$ in which the matrix was set up in the coupled basis $\boldsymbol{I}+\boldsymbol{J}=\boldsymbol{F}$ and diagonalized in blocks of *F*. $\boldsymbol{H_R}$ is the Watson's asymmetric reduced Hamiltonian in the I^r representation truncated after quartic terms of angular momentum.[12] $\boldsymbol{H_Q}$ is the operator describing the Cl-nuclear quadrupole coupling.[13] The associated observable spectroscopic quantities are the elements $\chi_{\alpha\beta}$ of the quadrupole coupling tensor, which are linearly related to the electric field gradient at the Cl nucleus with respect to the principal inertial axis system of the complex [Eq. (1), where eQ is the Cl-nuclear quadrupole moment].

$$\chi_{\alpha\beta} = -\left(\frac{eQ}{h}\right)\frac{\partial^2 V}{\partial\alpha\partial\beta} \quad (\alpha, \beta \text{ to be permuted over } a, b, c) \tag{1}$$

Rotational constants, quartic centrifugal distortion constants, and the three independent quadrupole coupling constants χ_{aa}, $(\chi_{bb}-\chi_{cc})$, and χ_{ac} (equatorial) or χ_{ab} (axial) were fitted simultaneously using the program of Pickett.[14] Since there were not enough data, the centrifugal distortion constant Δ_K had to be constraint to zero. The spectroscopic constants are given in Tables 3 and 4. A root mean square (rms) deviation (see Tables 3 and 4) comparable with the estimated accuracy of the frequency measurements was provided by releasing only one of the three possible off-diagonal elements of the nuclear quadrupole tensor (χ_{ac} or χ_{ab} for the equatorial or axial PMS···HCl respectively).

Structure

An analysis of the rotational parameters allows us to establish several important structural properties of the axial and equatorial PMS···HCl conformers. The planar moments P_b (equatorial) and P_c (axial) which only depend on the *b* or *c* coordinates respectively (see Tables 3 and 4 for definitions), are effectively unchanged upon isotopic substitution of Cl, H, or S atoms. This clearly shows that these atoms, which are

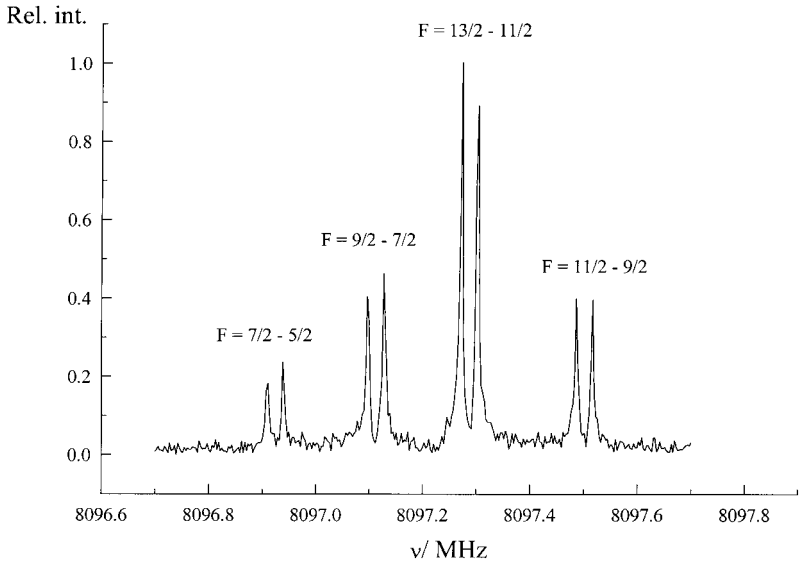

Figure 1. $5_{0,5} \leftarrow 4_{0,4}$ transition of the equatorial $C_5H_{10}{}^{32}S\cdots H^{35}Cl$ complex showing quadrupole coupling components splitted by Doppler effect.

0947-6539/99/0511-3294 $ 17.50+.50/0 *Chem. Eur. J.* **1999**, *5*, No. 11

Table 1. A selection of observed rotational transition frequencies (MHz) for the equatorial conformer of pentamethylene sulfide···HCl.

								$C_5H_{10}{}^{32}S\cdots H^{35}Cl$		$C_5H_{10}{}^{32}S\cdots H^{37}Cl$		$C_5H_{10}{}^{32}S\cdots D^{35}Cl$		$C_5H_{10}{}^{34}S\cdots H^{35}Cl$	
J'	K'_{-1}	K'_{+1}	J''	K''_{-1}	K''_{+1}	F'	F''[a]	*obs.*	*obs.-cal.*[b]	*obs.*	*obs.-cal.*[b]	*obs.*	*obs.-cal.*[b]	*obs.*	*obs.-cal.*[b]
3	1	2	2	0	2	5	4	6762.656	0.002						
						4	3	6759.745	0.000						
						3	2	6759.843	0.000						
5	0	5	4	0	4	7	6	8097.286	0.001	7872.728	0.001	8051.657	0.001	8080.012	0.001
						6	5	8097.500	−0.001	7872.881	0.001	8051.871	0.000	8080.208	0.000
						5	4	8097.111	−0.001	7872.571	0.000	8051.475	0.000	8079.821	0.001
						4	3	8096.922	0.000	7872.434	0.000	8051.287	0.000	8079.651	0.001
6	1	6	5	1	5	8	7	9616.680	0.000	9353.592	0.000	9564.114	0.001	9606.017	0.002
						7	6	9616.588	−0.001	9353.513	0.000	9564.019	0.001	9606.017	0.002
						6	5	9616.588	−0.001	9353.513	0.000	9564.024	−0.003	9605.920	−0.002
						5	4	9616.670	0.001	9353.584	0.002	9564.105	−0.002	9605.928	0.001
7	1	6	6	1	5	9	8	11470.776	0.000	11146.339	0.003	11403.492	0.000	11431.436	0.000
						8	7	11470.762	0.000	11146.320	0.003	11403.477	0.001	11431.414	0.000
						7	6	11470.486	−0.001	11146.102	0.003	11403.195	0.001	11431.138	−0.002
						6	5	11470.494	−0.001	11146.117	0.002	11403.204	−0.002	11431.155	−0.002
8	2	7	7	2	6	10	9	12965.981	0.002	12605.129	−0.003	12892.470	0.000		
						9	8	12965.787	0.000	12604.971	−0.001	12892.271	−0.001		
						8	7	12965.733	0.001	12604.924	−0.003	12892.215	−0.001		
						7	6	12965.912	0.002	12605.076	0.000	12892.399	0.001		
8	3	5	7	3	4	10	9	12980.354	−0.001			12906.169	0.001		
						9	8	12979.843	0.001			12905.661	0.002		
						8	7	12979.807	0.001			12905.612	0.003		
						7	6	12980.493	−0.002			12906.325	−0.002		
9	2	7	8	2	6	11	10	14648.115	0.002	14233.564	−0.001	14562.597	−0.002		
						10	9	14647.670	0.002	14233.227	−0.001	14562.148	−0.002		
						9	8	14647.638	0.002	14233.199	−0.002	14562.116	−0.002		
						8	7	14648.076	0.002	14233.531	−0.002	14562.558	−0.001		

[a] F: half integer rounded up to the next integer. [b] Obtained with the corresponding spectroscopic constants in Table 3.

Table 2. A selection of observed rotational transition frequencies (MHz) for the axial conformer of pentamethylene sulfide···HCl.

								$C_5H_{10}{}^{32}S\cdots H^{35}Cl$		$C_5H_{10}{}^{32}S\cdots H^{37}Cl$		$C_5H_{10}{}^{32}S\cdots D^{35}Cl$	
J'	K'_{-1}	K'_{+1}	J''	K''_{-1}	K''_{+1}	F'	F''[a]	*obs.*	*obs.* − *cal.*[b]	*obs.*	*obs.* − *cal.*[b]	*obs.*	*obs.* − *cal.*[b]
4	2	2	3	2	1	6	5	7755.173	0.003	7534.285	−0.002	7715.897	−0.002
						5	4	7752.491	−0.001	7532.123	0.002	7713.168	0.001
						4	3	7753.475	−0.001	7532.914	0.001	7714.169	−0.002
						3	2	7756.153	−0.003	7535.079	0.000	7716.902	−0.002
5	0	5	4	0	4	7	6	9609.333	0.001	9343.146	0.002	9560.865	0.001
						6	5	9608.975	0.001	9342.880	0.001	9560.499	0.000
						5	4	9608.521	0.001	9342.519	0.001	9560.036	0.000
						4	3	9608.878	0.000	9342.769	0.003	9560.400	−0.001
5	1	5	4	0	4	7	6	10240.935	0.001				
						5	4	10239.279	−0.001				
						4	3	10240.811	0.000				
6	1	6	5	1	5	8	7	11393.024	0.000	11077.561	0.001	11334.987	0.001
						7	6	11392.716	−0.001	11077.322	0.001	11334.673	0.001
						6	5	11392.350	−0.001	11077.032	0.000	11334.299	0.000
						5	4	11392.655	−0.001	11077.270	0.000	11334.611	0.001
6	3	3	5	3	2	8	7	11611.562	0.000	11282.573	−0.001	11552.790	−0.002
						7	6	11609.756	−0.001	11281.119	−0.001	11550.950	−0.001
						6	5	11610.161	−0.001	11281.444	−0.001	11551.362	0.000
						5	4	11611.960	−0.001	11282.892	−0.003	11553.196	−0.003
7	1	6	6	1	5	9	8	13697.262	−0.001	13310.756	−0.002	13628.669	0.000
						8	7	13696.960	−0.002	13310.529	−0.003	13628.362	0.000
						7	6	13696.875	−0.002	13310.458	−0.002	13628.276	0.000
						6	5	13697.174	−0.002	13310.681	−0.003	13628.580	0.000
8	2	7	7	2	6	10	9	15425.026	−0.001	14993.371	0.001	15347.113	0.000
						9	8	15424.576	0.001	14993.019	0.001	15346.653	0.000
						8	7	15424.510	0.001	14992.963	0.000	15346.584	0.000
						7	6	15424.955	−0.001	14993.314	0.001	15347.041	0.000

[a] F: half integer rounded up to the next integer. [b] Obtained with the corresponding spectroscopic constants in Table 4.

Table 3. Spectroscopic constants for equatorial pentamethylene sulfide···HCl.

	$C_5H_{10}{}^{32}S\cdots H^{35}Cl$	$C_5H_{10}{}^{32}S\cdots H^{37}Cl$	$C_5H_{10}{}^{32}S\cdots D^{35}Cl$	$C_5H_{10}{}^{34}S\cdots H^{35}Cl$
A [MHz]	2598.1652(31)[a]	2591.996(43)	2593.412(51)	2560.15(14)
B [MHz]	828.99756(44)	805.10345(35)	823.94695(49)	825.10216(58)
C [MHz]	792.71763(43)	771.38095(31)	788.53727(47)	792.74241(48)
P_b[b] [uÅ^2]	111.2072(13)	111.2094(28)	111.2069(32)	111.2015(67)
Δ_J [kHz]	0.59496(90)	0.57018(80)	0.5890(10)	0.5842(20)
Δ_{JK} [kHz]	−1.8578(85)	−1.812(21)	−1.883(10)	[−1.8578][d]
Δ_K [kHz]	[0.0][c]	[0.0][c]	[0.0][c]	[0.0][c]
δ_J [kHz]	−0.04423(93)	−0.0415(11)	−0.0452(11)	−0.0485(24)
δ_K [kHz]	−0.53(14)	[−0.53][d]	−0.35(17)	[−0.53][d]
χ_{aa} [MHz]	−20.156(28)	−16.261(46)	−20.556(35)	−20.18(11)
$(\chi_{bb}-\chi_{cc})$ [MHz]	32.313(46)	25.02(17)	32.92(15)	32.20(22)
$\lvert\chi_{ac}\rvert$ [MHz]	38.67(29)	30.74(41)	39.51(30)	[38.67][d]
N[e]	164	114	147	51
J max.	10	10	10	9
σ[f] [kHz]	1.4	1.5	1.7	1.4
χ_{xx}[g] [MHz]	26.19(29)	20.98(40)	26.79(30)	–
χ_{yy} [MHz]	26.235(37)	20.64(11)	26.738(93)	–
χ_{zz} [MHz]	−52.42(29)	−41.62(40)	−53.53(30)	–
α_{az}[h]	39.843(36)	39.529(72)	39.843(36)	–

[a] Standard error in parentheses in units of the last digit. [b] $P_b=(I_a-I_b+I_c)/2=\Sigma m_i b_i^2$. Conversion factor: 505379.1 MHz uÅ^2. [c] Parameter kept fixed in the fit. [d] Parameters fixed to the $C_5H_{10}{}^{32}S\cdots H^{35}Cl$ value. [e] Number of fitted quadrupole components. [f] Root mean square (rms) deviation of the fit. [g] Principal quadrupole coupling constants. [h] Angle, in degrees, between the *a* principal inertial axis and the *z* gradient field axis.

Table 4. Spectroscopic constants for axial pentamethylene sulfide···HCl.

	$C_5H_{10}{}^{32}S\cdots H^{35}Cl$	$C_5H_{10}{}^{32}S\cdots H^{37}Cl$	$C_5H_{10}{}^{32}S\cdots D^{35}Cl$
A [MHz]	1976.0638(42)[a]	1974.552(16)	1974.098(15)
B [MHz]	996.47280(46)	967.74215(49)	991.50923(48)
C [MHz]	935.95958(38)	910.24159(39)	931.14732(39)
P_c[b] [uÅ^2]	111.4801(13)	111.4785(21)	111.4816(20)
Δ_J [kHz]	0.7305(19)	0.6972(20)	0.7197(20)
Δ_{JK} [kHz]	2.346(15)	2.309(18)	2.286(15)
Δ_K [kHz]	[0.0][c]	[0.0]	[0.0]
δ_J [kHz]	0.0915(13)	0.0831(14)	0.0905(14)
δ_K [kHz]	−1.509(93)	−1.46(12)	−1.39(11)
χ_{aa} [MHz]	−29.424(23)	−23.561(21)	−30.021(19)
$(\chi_{bb}-\chi_{cc})$ [MHz]	−22.030(51)	−16.978(82)	−22.545(80)
$\lvert\chi_{ab}\rvert$ [MHz]	37.0(53)	26.4(30)	36.2(53)
N[d]	133	122	132
J max.	9	9	9
σ[e] [kHz]	1.6	1.6	1.6
χ_{xx}[f] [MHz]	27.7(49)	19.5(27)	26.8(49)
χ_{yy} [MHz]	25.727(37)	20.270(52)	26.283(50)
χ_{zz} (MHz)	−53.4(49)	−39.8(27)	−53.1(49)
α_{az}[g]	32.9(17)	31.5(15)	32.5(18)

[a] Standard error in parentheses in units of the last digit. [b] $P_c=(I_a+I_b-I_c)/2=\Sigma m_i c_i^2$. Conversion factor: 505379.1 MHz u Å^2. [c] Parameters in square brackets were kept fixed in the fit. [d] Number of fitted quadrupole components. [e] rms deviation of the fit. [f] Principal quadrupole coupling constants. [g] Angle, in degrees, between the *a* principal inertial axis and the *z* gradient field axis.

involved in the hydrogen bond, lie in the *ac* (equatorial) or *ab* (axial) principal inertial planes of the complexes. Furthermore, these quantities are almost identical to the planar moment $P_b=111.19387(76)$ uÅ^2 [9] of free PMS. Since the *ac* inertial plane of PMS is the molecular symmetry plane, these results are strong evidence that both *ac* (equatorial) and *ab* (axial) inertial planes are also molecular symmetry planes for the complex. The small differences between either P_b or P_c of each conformer and P_b of PMS can be explained by taking into account the additional contributions of the intermolecular vibrations to the zero-point motion of the dimer. We conclude therefore that the axial and equatorial PMS···HCl complexes have C_s symmetry, with the HCl subunit lying in the symmetry plane of PMS (see Figure 2). The failure of the search for c-type (axial) or b-type (equatorial) transitions reinforces this conclusion. The location of HCl in the symmetry plane is also consistent with the nonzero values of the χ_{ac} (equatorial) or χ_{ab} (axial) off-diagonal elements of the Cl-nuclear quadrupole coupling tensor and with the fact that the ratios $^{35}\chi_{bb}/^{37}\chi_{bb}=1.270(9)$ for the equatorial and $^{35}\chi_{cc}/^{37}\chi_{cc}=1.269(5)$ for the axial are in good agreement with the theoretical value $^{35}Q/^{37}Q=1.26878(15)$.[15] The changes in the rotational constants on the isotopic substitutions of H(D) and ^{35}Cl (^{37}Cl) indicate that only geometries of the hydrogen-bonded type in which HCl is the proton donor need to be considered.

In order to determine the structure of the complexes from the rotational constants of Tables 3 and 4, we assumed that the structures of PMS[8, 9] and HCl[11] remain unchanged upon complexation. It proved impossible to determine the position of the hydrogen atom because of the small contribution that this atom makes to the rotational constants. Initially, a first fit was performed to determine preliminary values for the S···Cl distance and the angle ϕ between the S···Cl line and the line bisecting the C-S-C angle considering a collinear arrangement of the S···H–Cl system. However, further information about the position of the hydrogen atom is provided if the angle α_{az} between the HCl axis direction *z* and the *a* inertial axis is available. A good approximation to this angle can be obtained from the components of the Cl-nuclear quadrupole coupling tensor through[16] Equation 2 in those cases where *ab* (axial) is the molecular symmetry plane. A similar expression applies when *ac* (equatorial) is the symmetry plane. Values of α_{az} so determined for the different isotopomers of the axial and equatorial conformers are collected in Tables 3 and 4.

$$\alpha_{az}=\tfrac{1}{2}\tan^{-1}[-2\chi_{ab}(\chi_{aa}-\chi_{bb})^{-1}] \quad (2)$$

0947-6539/99/0511-3296 $ 17.50+.50/0 *Chem. Eur. J.* **1999**, *5*, No. 11

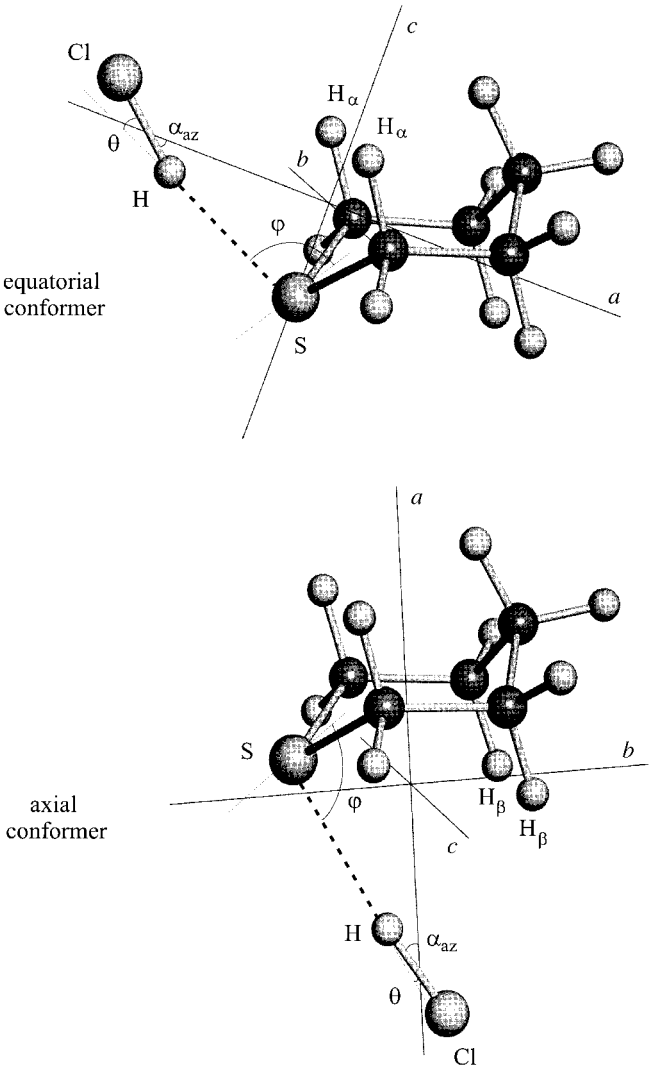

Figure 2. Structures of axial and equatorial conformers of pentamethylene sulfide···HCl.

The hydrogen bond structural parameters for each conformer have been finally obtained by iterative least-squares fits of the rotational constants for all observed isotopic species with α_{az} constrained to the values calculated for the parent species of axial and equatorial forms. In this way, precise determination of the $r(S\cdots Cl)$ distance and the angle ϕ were then possible. The results are given in Table 5 along with the derived values for the hydrogen bond length $r(S\cdots H)$, the angle φ between the S···H bond and the line bisecting the C-S-C angle, and the angle θ of deviation of the S···H–Cl nuclei from collinearity. The resulting geometry is drawn to scale in Figure 2.

Table 5. Hydrogen bond structural parameters of pentamethylene sulfide···HCl (see Figure 2).

	Axial	Equatorial
$r(S\cdots Cl)$	3.63(4)[a] Å	3.44(2) Å
ϕ	98.3(11)°	91.8(9)°
$r(S\cdots H)$	2.35(8) Å	2.19(5) Å
φ	100.(2)°	98.1(10)
θ	6.(3)°	17.2(2)°

[a] Standard errors in parentheses in units of the last digit.

Discussion

A first rationalization of the structure of the axial and equatorial forms can be made using a simple electrostatic model. Thus the nearly equal values of the φ angles for the axial and the equatorial forms (see Table 5 and Figure 2) can be understood in terms of an interaction between the electrophilic region $^{\delta+}$H of the HCl molecule with the high electron density regions in the acceptor molecule. In PMS these regions may be identified with the domains of the sulfur atom nonbonding pairs. In this way, the direction of the HCl molecule in the PMS···HCl complexes acts as a probe for the direction of the nonbonding pairs at S.

Another interesting point to discuss concerning the structures of axial and equatorial forms is the nonlinearity of the system S···H–Cl involved in the hydrogen bond. Whereas for the axial form is observed a nearly collinear arrangement ($\theta = 6(3)°$, see Table 5), the equatorial form shows a pronounced deviation from collinearity ($\theta = 17.2(2)°$). The nonlinearity of hydrogen bonds in related dimers[3, 10, 16] has been interpreted as arising from secondary interactions between the Cl atom and the nearest H atoms of the methylene groups in the ring, that is the H atoms of the α methylene groups in the equatorial form and the corresponding ones of the β methylene groups in the axial conformer (see Figure 2). The distances between the atoms presumably involved in these interactions have been calculated to be 3.34 Å (equatorial) and 3.12 Å (axial). These values are comparable to those reported for tetrahydrothiophene···HCl.[3] On this basis the small nonlinearity observed for the axial form does not exclude the existence of secondary hydrogen bond interactions.

A second point of interest is the intensity ratio (ax:eq ≈ 1:4) observed in the a-type rotational spectra of the axial and equatorial conformers. It has been reported[17] that the observation of different conformers in a supersonic expansion sometimes has a dependence on the carrier gas. Heavier carrier gases may produce a relaxation from higher energy forms to the lower one when the barrier to interconversion between them is lower than a certain limit (let say $\approx 400\ cm^{-1}$[17]). For PMS···HCl this effect is not observed. The ratio between the axial and the equatorial conformers remains qualitatively unaltered even when the carrier gas is changed. This may be attributed to the existence of a barrier to interconversion between the axial and equatorial forms high enough to inhibit relaxation. The difference in the intensity of the rotational spectra of the conformers could not be caused by different values of the electric dipole moments for both conformers since rough dipole moment calculations gave similar values for the μ_a dipole moment components. Thus, the observed intensities indicate that the equatorial form is the most stable one. The shorter S···H distance (of about 0.2 Å) for the equatorial conformer (see Table 5) points to the same conclusion if we accept that a shortening in the bond length can be related to an increase in bond strength.

This result is strikingly different from what has been observed for the related complex tetrahydropyran···HCl,[10] where the axial form was found to be the most stable one. An open question is how the second-order interaction contributes

to the axial and equatorial conformational preference of hydrogen bonding. While in the case of tetrahydropyran $\cdots$ HCl[10] evidence was found of the nonexistence of significant secondary interactions for the equatorial conformer, in PMS $\cdots$ HCl the noticiable nonlinearity of the atoms involved in the hydrogen bond strongly indicates the existence of second-order interactions which may favor the equatorial form of the complex.

Experimental Section

All measurements were performed in the frequency range 6 – 18 GHz using the molecular beam Fourier transform microwave spectrometer which was described earlier.[18] The isotopic species ^{35}Cl, ^{37}Cl, ^{32}S, and ^{34}S were observed in their natural abundance. The assignment of the lines to the complexes was confirmed by establishing that both PMS and HCl had to be present in the adiabatic expansion for their observation. Gas mixtures of about 1 % of PMS (Aldrich) and 4 % of HCl (Aldrich) or DCl (Euriso-top) in Ar or He (total pressure 1 – 1.5 bar) were pulsed into an evacuated Fabry – Perot cavity to generate dimers in high number density by virtue of a very low effective temperature in the expanding gas. A delayed microwave pulse then polarizes the dimer molecules when they are in collisionless expansion into the cavity. The molecules subsequently emit coherent radiation at their rotational transition frequencies which are obtained after Fourier transformation of the time domain signal. Since the nozzle (General Valve, series 9) is mounted slightly off center behind one mirror, the gas pulse travels coaxially to the direction of propagation of the microwaves giving rise to a Doppler doublet for each transition line. Figure 1 provides an example of a typical transition collected for this study. The average frequency of each doublet gives the rest frequency of the molecular transition. The linewidth (FWHM) for a single line typically lies between 5 and 8 kHz. Frequency measurements are estimated to have an accuracy better of 5 kHz.

Acknowledgments

The authors would like to thank the Dirección General de Enseñanza Superior (DGES Grant PB96-0366) and the Junta de Castilla y León (JCL Grants VA51/96 and VA04/98) for funds. M. E. S. gratefully acknowledges an FPI grant from the Ministerio de Educación y Cultura.

[1] G. C. Pimentel, A. C. McClellan, *The hydrogen bond* (Ed.: L. Pauling), Freeman, San Francisco, **1960**; S. N. Vinogradov, R. H. Linnell, *Hydrogen bonding*, van Nostrand Reinhold Co., New York, **1971**; J. A. Jeffrey, W. Saenger, *Hydrogen bonding in biological structures*, Springer, Berlin, **1991**; J. A. Jeffrey, *Introduction to hydrogen bonding*, University Press, Oxford, **1997**.
[2] See, for example, J. M. Hollas, *Jet Spectroscopy and Molecular Dynamics* (Eds.: J. M. Hollas, D. Phillips), Chapman & Hall, Glasgow, **1995**.
[3] M. E. Sanz, J. C. López, J. L. Alonso, *J. Phys. Chem. A* **1998**, *102*, 3681 – 3689.
[4] M. E. Sanz, J. C. López, J. L. Alonso, *Chem. Phys. Lett.* **1998**, *288*, 760 – 766.
[5] J. C. López, J. L. Alonso, F. J. Lorenzo, V. M. Reyon, J. A. Sordo, *J. Chem. Phys.*, in press.
[6] J. L. Alonso et al., unpublished results.
[7] A. C. Legon, D. J. Millen, *Chem. Soc. Rev.* **1987**, *16*, 467 – 498.
[8] R. W. Kitchin, T. B. Malloy, Jr., R. L. Cook, *J. Mol. Spectrosc.* **1975**, *57*, 179 – 188.
[9] J. C. López, J. L. Alonso, R. M. Villamañán, *J. Mol. Struct.* **1986**, *147*, 67 – 76.
[10] S. Antolínez, J. C. López, J. L. Alonso, *Angew. Chem.* **1999**, *111*, 1889 – 1891; *Angew. Chem. Int. Ed.* **1999**, *38*, 1772 – 1774.
[11] F. C. de Lucia, P. Helminger, W. Gordy, *Phys. Rev. A.* **1971**, *3*,1849 – 1857.
[12] J. K. G. Watson in *Vibrational Spectra and Structure*, *Vol. 6* (Ed.: J. R. Durig), Elsevier, Amsterdam, **1977**, pp. 1 – 89.
[13] W. Gordy, R. L. Cook, *Microwave Molecular Spectra*, Wiley, New York, **1984**, chapter 9 and 14.
[14] H. M. Pickett, *J. Mol. Spectrosc.* **1991**, *148*, 371 – 377.
[15] W. Gordy, R. L. Cook, *Microwave Molecular Spectra*, Wiley, New York, **1984**, p. 861.
[16] A. C. Legon, *Faraday Discuss.* **1994**, *97*, 19 – 33.
[17] R. S. Ruoff, T. D. Klots, T. Emilsson, H. S. Gutowsky, *J. Chem. Phys.* **1990**, *93*, 3142 – 3150.
[18] J. L. Alonso, F. J. Lorenzo, J. C. López, A. Lesarri, S. Mata, H. Dreizler, *Chem. Phys.* **1997**, *218*, 267 – 275.

Received: May 6, 1999 [F1770]

  0947-6539/99/0511-3298 $ 17.50+.50/0